

Research on fault location algorithm of TPSS Based on PSOA

Yunqian Jia ^{Corresp. 1}

¹ Shanghai Institute Of Technology, School of Railway Transportation, Shanghai, China

Corresponding Author: Yunqian Jia
Email address: 216151112@mail.sit.edu.cn

It is extremely important to research traction power supply system (TPSS) protection technology in order to ensure the safe operation of urban rail transit. A TPSS includes rails, return cables, rail potential limiting devices, one-way conducting devices, drainage cabinets, ballast beds, and tunnel structural reinforcements. In urban rail transit, on the basis of the dynamic characteristics of the TPSS, a fault location algorithm based on particle swarm optimization algorithm (PSOA) is developed. An evaluation of multi-point monitoring data is proposed based on fuzzy processing of the average value of polarization potential forward deviation and multi-attribute decision-making. Monitoring points and standard comparison threshold values are determined by the distribution law of stray currents. In conjunction with the actual project, the model is trained using field measured data. Based on the results, TPSSOA is able to achieve optimal discharge current control, reduce network losses and improve power quality. Moreover, the reconstruction results demonstrate the high usability of the proposed method, which will provide guidance to design the TPSS in the future.

1 Research on fault location algorithm of TPSS Based on PSOA

2

3 Yunqian Jia*

4 Shanghai Institute Of Technology, School of Railway Transportation, Shanghai 201400, China.

5 Correspondence: Yunqian Jia; 216151112@mail.sit.edu.cn

6

7 Abstract

8 It is extremely important to research traction power supply system (TPSS) protection
9 technology in order to ensure the safe operation of urban rail transit. A TPSS includes rails, return
10 cables, rail potential limiting devices, one-way conducting devices, drainage cabinets, ballast beds,
11 and tunnel structural reinforcements. In urban rail transit, on the basis of the dynamic
12 characteristics of the TPSS, a fault location algorithm based on particle swarm optimization
13 algorithm (PSOA) is developed. An evaluation of multi-point monitoring data is proposed based
14 on fuzzy processing of the average value of polarization potential forward deviation and multi-
15 attribute decision-making. Monitoring points and standard comparison threshold values are
16 determined by the distribution law of stray currents. In conjunction with the actual project, the
17 model is trained using field measured data. Based on the results, TPSSOA is able to achieve
18 optimal discharge current control, reduce network losses and improve power quality. Moreover,
19 the reconstruction results demonstrate the high usability of the proposed method, which will
20 provide guidance to design the TPSS in the future.

21 **Keywords:** traction power supply; machine learning; particle swarm optimization algorithm; fault
22 location

23

24 1 Introduction

25 Urban development has been restricted by the bottleneck problem of urban internal traffic
26 development as the economy and urbanization have grown rapidly. Due to its advantages of large
27 traffic volumes, low energy consumption, safety, fast and punctual comfort, Large and medium-
28 sized cities now rely on urban rail transit to alleviate traffic congestion. Nearly 120 cities around
29 the world have built urban rail transit systems within the past 100 years, and the operating mileage
30 of these systems exceeds 7000 kilometers, according to incomplete statistics. Electric traction
31 system can be divided into DC electric traction and AC electric traction. TPSS requires constant
32 starting torque and good speed regulation characteristics. Due to the volume and cost of high-
33 power converter, AC electric traction is not suitable to be installed separately in each traction
34 locomotive. However, DC series excitation motor can better meet these requirements, so DC
35 traction system is mostly adopted [1-2]. DC traction system is widely used in urban rail transit
36 system, because it has the following three characteristics: (1) urban rail transit system
37 (underground tunnel or light rail) mostly runs through the urban area, and the corridor space of
38 electric traction line is limited;(2) As a traction load, locomotive has the characteristics of high
39 density, short running distance and frequent changes of running state. Locomotive operation can
40 be divided into three states: starting, idling and braking. Under different states, the system current
41 changes greatly with high frequency. The traction current is large when starting, small when idling,
42 and reverse when braking;(3) In order to increase transport capacity, on-board equipment should
43 be simplified as far as possible [3].

44 As an important part of TPSS, the reflux system and its influence have been paid more
45 attention in the world. A gratifying progress is being made on DC traction power supply return

46 systems due to the rapid development of urban rail transit. As much as possible, rail leakage current
47 should be reduced to eliminate stray current from the source. There is still widespread use of many
48 protection principles and measures summarized by Yang et al. [4]. Among the specific protection
49 measures outlined by Chen et al. [5] are: maintaining a high level of rail ground insulation. Adopt
50 effective grounding and connection scheme. The upper and lower rails are connected by welding.
51 The stray current collection system should be established reasonably. Reduce the resistance of
52 return rail. Reduce the distance between traction posts. Track and structural steel are isolated,
53 especially when ballast bed drainage network is used. Ensure that the track is dry and the drainage
54 is timely. The necessity of monitoring stray current leakage outside the system is proposed. In
55 addition, high rail potential will cause a lot of stray current leakage, the comprehensive measures
56 discussed by Chen et al. [6] included increasing the voltage on the traction network, increasing the
57 cross-sectional area of return rails, welding long rails, and reducing the distance between
58 substations. Due to the short circuit between the track and the ground, the original insulation
59 protection measures designed on the line will lose the protection function. Taking effective
60 measures for active treatment is therefore necessary to address the phenomenon.

61 Many cities have the above problems with their subway operations, and the relevant
62 protection technology needs to be improved and solved. It is extremely important to research TPSS
63 protection technology in order to ensure the safe operation of urban rail transit. On the basis of the
64 dynamic characteristics of the TPSS, a TPSSOA algorithm is developed.. The exhaust flow control
65 is equivalent to duty cycle adjustment based on the dynamic flow drainage method of multi-point
66 monitoring data. The predictive model can effectively control discharges after being trained on
67 field data, and using the actual project to implement drainage control.
68

69 **2 Related works**

70 Chen et al. [6] analyzed the characteristics of DC TPSS. Based on the assumption that the rail
71 ground insulation is uniformly distributed, it is established that rail resistance and rail ground
72 transition resistance are variables in a continuous distribution model and relevant formulas are
73 derived and analyzed. Considering the influence of ballast reinforcement structure, the continuous
74 distribution model of rail, structure and earth is established. According to Lin et al. [7], the
75 simplified boundary conditions were adopted in the theoretical analysis, because the parameters
76 were assumed to have a continuous distribution in the actual situation. The theoretical calculation
77 and simulation results obtained could not completely correspond to the actual situation. Therefore,
78 the various analysis results at this stage can only be used as the reference for qualitative analysis,
79 and there is a big gap between the accurate calculation of the distribution and influence of each
80 parameter. As a result of their work, Dai et al. [8] have developed the discrete distribution model,
81 given the software program based on one car and one section, and conducted simulation analyses.
82 They have also calculated the effect of subway stray current using finite element method, which is the basis for
83 determining the protection range of stray current and quantifying the influence degree of subway stray current
84 on surrounding buried metal structures. The traditional circuit theory has encountered many difficulties in the
85 analysis of reflux system. Many scholars try to use other theoretical models to analyze the reflux system.
86 Nezevak et al. [9] developed a model of multi locomotive and multi section using the node equation matrix
87 method, conducted simulation analysis, and verified the simulation results on the ground. Based on the electric
88 field theory, hemispherical electrode was used to solve the electric field distribution under the influence of stray
89 current, so as to calculate the leakage current in buried metal and predict the corrosion of stray current to buried
90 metal. Zhang et al. [10] derived analytical formulas for the track voltage, track current, stray current, rail ground
91 transition resistance, and other parameters under the continuous and discrete methods, and carried out simulation
92 analyses.

93 On the basis of a section of track, Yuan et al. [11] derived the relationship between rail ground voltage and

94 stray current. When there is a buried metal structure near the track, the potential gradient of leakage current is
 95 calculated by using field theory. When the parallel or crossed buried metal is in the electric field,
 96 there will be potential difference and stray current corrosion. The limitations of practical
 97 application such as discontinuous transition resistance and uneven soil resistivity are discussed.
 98 According to Lin et al. [12], stray current distribution in DC traction systems is characterized by
 99 time variations. As a return path, Wang et al. [13] considered a rail as a ferromagnetic conductor
 100 with an irregular cross-section. When the traction current changes sharply, it is necessary to
 101 analyze the influence of its transient characteristics on the rail potential. Taking the independent
 102 rail as an example, the frequency-domain transient characteristic parameters are calculated and the
 103 transient parameter model is established. The influence of frequently changing traction current on
 104 rail transient parameters is discussed.

105

106 3 TPSSOA scheme

107

108 3.1 PSOA

109

110 Based on research on bird predation behavior, Kennedy and Eberharty developed PSOA.
 111 Birds can't know the exact location of food if there is only one piece in their foraging range, but
 112 they can feel the distance between themselves and the food when foraging in a flock. Therefore, if
 113 you want to spend the least time to find food, the birds can follow the nearest bird to find food. In
 114 the PSOA, the bird swarm is the particle swarm, and a single bird corresponds to a single particle.
 115 The process of PSOA solving the optimization problem is accompanied by the updating of particle
 116 velocity and position. In the process of algorithm optimization, each particle has its own speed and
 117 position, and updates the speed and position independently.

118 At the same time, the particles will constantly adjust the search direction according to their
 119 own experience and the experience of other particles, and finally realize the search of the optimal
 120 value.

121

122

123 The schematic diagram of DG in orbit is shown in Figure 1. As a final conclusion, the
 124 population is positioned optimally depending on the optimization problem. The updating formulas
 125 of velocity and position are shown in equations (1) and (2)

126

$X_{id}^{k+1} = X_{id}^k + V_{id}^{k+1}$	(1)
$X_{i+1} = r_1 k(1 - V_{id})(V_{id} - k + 1)$	
$V_{id}^{k+1} = wV_{id}^k + c_1 r_1 (P_{id} - X_{id})$	(2)

127

128 In the present optimal value formula, X_{id}^{k+1} for the first time $k + 1$, the velocity and position
 129 of the second iteration, w is the inertia weight, V_{id} , X_{id} . The velocity and position of the second
 130 iteration; c_1 , c_2 are the acceleration factor, which is usually greater than 0; r_1, r_2 are interval $[0, 1]$
 131 . The random constant in the P_{id}, X_{id} are the optimal positions of individuals and populations
 132 respectively. Many scholars have made efforts to improve IPSO, and put forward an improved
 133 method to make the inertia weight decrease linearly. In order to improve the algorithm's search

134 ability, the compression factor is introduced, and the inertia weight strategy of nonlinear
 135 decreasing is introduced. The above-mentioned improvement measures can solve simple
 136 optimization problems, but when the problems are complicated, the optimization effect will be
 137 greatly reduced. To solve this problem, this paper studies the learning factors in PSO c_1 , c_2 . And
 138 inertia weight w . Optimization is performed on three parameters that significantly influence
 139 algorithm performance. The improved inertia weight is shown in formula (3)
 140

$$c_1 = c_{1max} + c_{1min} \sin(1-t)\pi \quad (3)$$

141 c_1 is the current fitness value, c_{1max} is the minimum fitness value, c_{1min} is the average fitness
 142 value. It represents the number of iterations that have been carried out so far and the maximum
 143 number of iterations that can be carried out. In this way, with the continuous iteration of the
 144 algorithm, w In the iterative process, the value of the fitness value is dynamically adjusted to
 145 improve its optimization performance. In addition, this paper also adopts the strategy of
 146 dynamically adjusting the acceleration factor based on the change of fitness value. It needs to be
 147 mapped to chaotic sequences Z_i . The mapping process is shown in equation (4)
 148

$$Z_i = Y_i - \frac{Y_{min}}{Y_{imax} - Y_{imin}} \quad (4)$$

150 Final chaotic variable Y_i is required for the generation process, as shown in equation (5)
 151

$$Y_i = Z_i(Y_{imax} - Y_{imin}) + Y_{imin} \quad (5)$$

153 3.2 Specific scheme of TPSSOA

154 It is commonly used to use integer values of 0-0 as a parameter in urban rail transit models.
 155 The simple power supply network is shown in Figure 2.
 156

157 Taking this as an example, because the network only has the main power supply for power
 158 supply, the current direction is that the system power supply flows to the load. When the fault
 159 occurs in the section, the traction network corresponding to the section monitors the fault current
 160 passing through. Thus, for the switch with fault over-current, the status value of the corresponding
 161 node is "1", whereas for the switch without fault over-current, the status value is "0". That is to
 162 say, for a single switch node, only the downstream section fault needs to be considered.
 163

164
 165 (1) TPSSOA firstly collects and uploads the fault current information in real time by using
 166 traction network, and realizes the conversion from fault current information to fault vector by using
 167 improved fault integer programming model, that is, according to the actual situation of fault current
 168 direction detected by traction network, it can be converted into "1", "- 1" or "0".
 169

170 (2) Then the switch function of urban rail transit with rail transit is constructed, and the
 171 equivalent fault vector of fault location is calculated. The equivalent fault vector is input into the
 172 algorithm, the population dimension of PSO and the coding length of genetic algorithm are set as

173 the total number of feeder sections, and the evaluation function is the objective function of the
174 algorithm.

175 (3) Finally, the optimal particle position of PSO is output to realize the fault section location.
176 In this paper, an adaptive PSO is proposed by dynamically improving the fitness value of the
177 PSOA. Combined with the adaptive genetic algorithm, the search iteration ability of the adaptive
178 genetic PSOA is proposed.

179 The corresponding flow chart is shown in Figure 3. The specific steps of fault location using
180 the improved algorithm are as follows:

181 (1) There were set parameters such as the number of iterations and the size of the population.

182 (2) Initiate the population information and construct the switch function and evaluation
183 function.

184 (3) Calculate the fitness function value and perform the genetic algorithm selection.

185 (4) We calculate the crossover probability of genetic algorithms and perform crossover
186 operations.

187 (5) The mutation probability of genetic algorithm is calculated and mutation operation is
188 performed.

189 (6) Judge whether the current fitness value meets the convergence condition, and if so,
190 execute the next step. Otherwise, return to step (3).

191 (7) Output population information and initialize the velocity and position of particles.

192 (8) The current fitness value is solved and the velocity and position of particles are updated.

193 (9) In the case of a convergence condition being met, execute the next operation if it has been
194 met..

195 (10) The optimal particle output is the fault section.

196

197

198 When TPSSOA determines a fault point and its opposite bus, it compares the reflected waves
199 by polarity. Wavelet analysis is used to identify and extract the fault signal, and the structure and
200 operation characteristics of Metro DC traction power supply system are different from those of
201 high-voltage transmission lines. In general, there are two incoming lines and four feeders
202 connected with the up and down lines in the left and right sections respectively. Moreover, the
203 change of traction load will also bring interference to the direction discrimination of traveling
204 wave. If the discrimination is wrong, it will cause great ranging error. Therefore, TPSSOA
205 combines with fault analysis method, calculates the fault location by the optimized fault location
206 algorithm proposed above, and when the reflection waves of a fault point and the opposite bus
207 arrive at the measuring end, that is the time interval when the reflected wave of the fault point
208 arrives. In the area, the accurate arrival time of fault point reflection wave and opposite bus
209 reflection wave is determined respectively, and then the fault location is carried out by substituting
210 it into the formula. Among them, the fault analysis method is applicable to any section of data in
211 the whole instantaneous process, which requires a small amount of data, and can share the data
212 source with the traveling wave method without additional workload in data acquisition.

213

214 **4 Model simulation and result analysis**

215

216 The reference voltage of rail transit traction system used in this experiment is 18kV, the
217 reference power is 10mVA, and the network load is $3715 + j2300$ kVA. The Parameters of
218 TPSSOA algorithm is shown in table 1.

219

220 When DG is not connected, when there is no DG in urban rail transit, the status values of the
221 switch are only "0" and "1". If there is high temperature, humidity and other harsh conditions, the
222 fault information collected may be different from the actual value. Therefore, the information
223 distortion is considered in this experiment. The simulation results are shown in Table 2.

224 It can be seen from the results in Table 2 that the fault area can also be accurately located
225 when multiple sections are in fault at the same time and the fault information is not accurate. At
226 the same time, the fault section can be accurately determined even if the fault information of
227 multiple feeder sections is not accurate. As a result of the simulations, the fault location method
228 proposed can dynamically adapt to the flow of DGs into and out of the fault, and the experimental
229 results are not disturbed by distorted information. In order to reflect the advantages of the improved
230 algorithm in fault location, this paper compares the TPSSOA algorithm with the improved PSOA
231 (IPSO) after introducing the compression factor and linear decreasing inertia weight. The formula
232 of linear decreasing inertia weight and compression factor is shown in formula (6)
233

$$w = w_{max} - (w_{max} - w_{min})T_{max} \quad (6)$$

234

235 Where, w_{max} is the compression factor and $T_{max} = C_1$. Different fault conditions are set, and
236 simulation and comparative analysis are carried out in terms of rapidity. DG grid connection
237 coefficient is set as $[k1, k2, k3] = [11000110111110]$.

238 The iterative curves of the two algorithms in fault location are shown in Figure 4 (No
239 distortion in single section) and Figure 5 (No distortion in multiple sections). The horizontal axis
240 is the number of iterations and the vertical axis is the fitness value. The default fault location is
241 feeder section (1), and the fault information has no distortion.

242

243 It can be seen from the results in Figure 4 that both algorithms can achieve minimum values
244 within the maximum number of iterations, but the speed of TPSSOA is the faster than IPSO. The
245 preset fault location is feeder section (2), and the fault information at switch (3) is distorted. It can
246 be seen from Figure 5 that IPSO falls into a local optimal value at the early stage of iteration. In
247 order to obtain the global optimal value, more iterations are needed. However, TPSSOA achieves
248 global extremum with less iterations. The comparison results show that IPSO algorithm can hardly
249 locate multiple section faults with a large amount of inaccurate information, and the accuracy of
250 single fault location is not high, so it is only suitable for simple urban rail transit. The TPSSOA
251 algorithm has high positioning accuracy and is hardly affected by the increase of fault section and
252 distortion information. In this paper, fault reconstruction experiments are used to demonstrate the
253 effectiveness of the method proposed. on urban rail transit without grid connected DG and urban
254 rail transit with different types of DG connected. Reconstruction of the fault leads to the restoration
255 of power supply in the non-fault area and a reduction of network losses. Compared with IPSO
256 algorithm, TPSSOA uses the improved algorithm to reconstruct the switch combination network
257 with lower loss and less time-consuming. In addition, voltage amplitudes and voltage distributions
258 are improving. At the same time, after fault reconstruction, the combination of (3) (4) (5) is
259 changed to (1) (2) (3) (5), the network loss is reduced from 111.6606kw to 72.4095kw, and the
260 minimum node voltage is also increased from 0.9342 to 0.9599. Compared with the fault
261 reconstruction scheme using IPSO algorithm, the reconstruction scheme using TPSSOA algorithm
262 can reduce more network loss and increase more voltage amplitude. In conclusion, IPSO is easy
263 to be disturbed by distorted information when using the above algorithm, and it falls into local

264 extremum many times in the whole iteration process, so it is only suitable for fault location of
265 simple urban rail transit. The TPSSOA proposed in this paper has strong anti-interference ability
266 for distortion information, and can quickly obtain global extreme value, so as to make accurate
267 identification of fault section. It has excellent fault tolerance and stability, and greatly improves
268 the search ability of the algorithm. It can be used in urban rail transit with DG

269

270 **5 Conclusion**

271

272 TPSS in urban rail transit are constantly evolving and improving, enhancing reliability and
273 operation economy, but also increasing the probability of failure, and network architectures are
274 becoming more complex. Due to limitations in existing fault location and recovery reconstruction
275 methods, this paper presents an algorithm based on PSO that improves the location model,
276 optimizes the PSO, and enables the algorithm to be more efficient in optimizing the location
277 model. An improved fault location method is developed, and DG grid connection and distortion
278 information are not affecting the experimental results of the fault location experiment. We
279 conclude that the proposed fault location method can reduce network losses and improve power
280 quality based on the reconstruction results.

281

282 **Conflicts of Interest**

283 The author declare that there are no conflicts of interest.

284 **Funding Statement**

285 This work received no funding.

286 **References**

287 [1] He X, Peng J, Han P, et al. A novel advanced traction power supply system based on
288 modular multilevel converter[J]. IEEE Access, 2019, 7: 165018-165028.

289 [2] Liu L, Dai N Y, Lao K W, et al. A co-phase traction power supply system based on
290 asymmetric three-leg hybrid power quality conditioner[J]. IEEE Transactions on Vehicular
291 Technology, 2020, 69(12): 14645-14656.

292 [3] Zhong Z, Zhang Y, Shen H, et al. Optimal planning of distributed photovoltaic generation
293 for the traction power supply system of high-speed railway[J]. Journal of Cleaner Production,
294 2020, 263: 121394.

295 [4] Yang X, Hu H, Ge Y, et al. An improved droop control strategy for VSC-based MVDC
296 traction power supply system[J]. IEEE Transactions on Industry Applications, 2018, 54(5): 5173-
297 5186.

298 [5] Chen M, Cheng Y, Cheng Z, et al. Energy storage traction power supply system and
299 control strategy for an electrified railway[J]. IET Generation, Transmission & Distribution, 2020,
300 14(12): 2304-2314.

301 [6] Chen Y, Tian Z, Roberts C, et al. Reliability and life evaluation of a DC traction power
302 supply system considering load characteristics[J]. IEEE Transactions on Transportation
303 Electrification, 2020, 7(3): 958-968.

- 304 [7] Lin S, Feng D, Sun X. Traction power-supply system risk assessment for high-speed
305 railways considering train timetable effects[J]. IEEE Transactions on Reliability, 2019, 68(3): 810-
306 818.
- 307 [8] Dai Y, Zhang L, Liu G, et al. Multi-VSM based fuzzy adaptive cooperative control
308 strategy for MVDC traction power supply system[J]. Journal of the Franklin Institute, 2021,
309 358(15): 7559-7585.
- 310 [9] Nezevak V, Cheremisin V, Shatokhin A. Assessment of energy intensity of the drive for
311 traction power supply system[C]//Energy Management of Municipal Transportation Facilities and
312 Transport. Springer, Cham, 2018: 524-538.
- 313 [10] Zhang G, Tian Z, Du H, et al. A novel hybrid DC traction power supply system integrating
314 PV and reversible converters[J]. Energies, 2018, 11(7): 1661.
- 315 [11] Yuan J, Xiao F, Zhang C, et al. Collaborative unbalance compensation method for
316 high-speed railway traction power supply system considering energy feedback[J]. IET Power
317 Electronics, 2019, 12(1): 129-137.
- 318 [12] Lin S, Chen X, Wang Q. Fault diagnosis model based on Bayesian network considering
319 information uncertainty and its application in traction power supply system[J]. IEEE Transactions
320 on Electrical and Electronic Engineering, 2018, 13(5): 671-680.
- 321 [13] Wang M, Yang X, Zheng T Q, et al. DC autotransformer-based traction power supply for
322 urban transit rail potential and stray current mitigation[J]. IEEE Transactions on Transportation
323 Electrification, 2020, 6(2): 762-773.

Figure 1

Figure 1. DG schematic diagram

The schematic diagram of DG in orbit is shown in Figure 1.

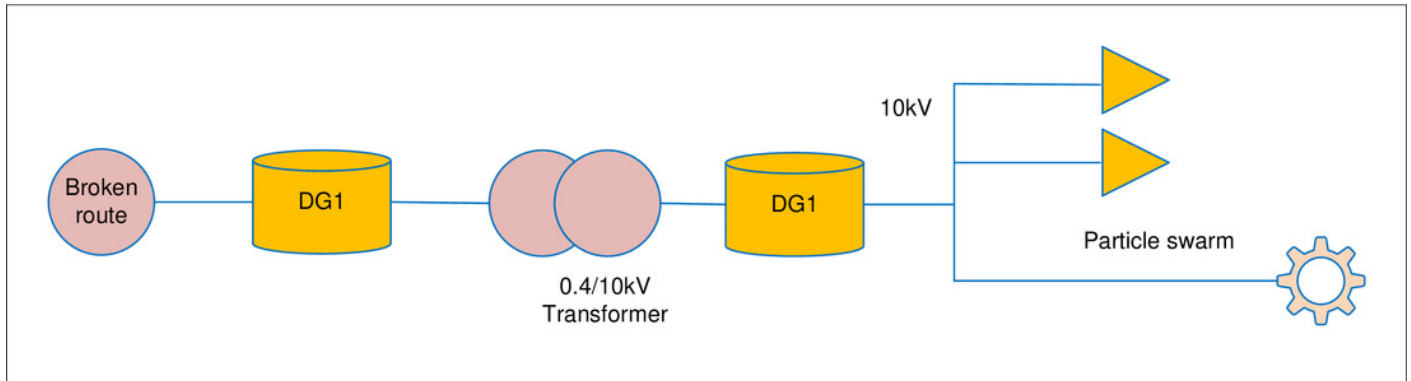


Figure 2

Figure 2. Schematic diagram of power supply network

It is commonly used to use integer values of 0-0 as a parameter in urban rail transit models. The simple power supply network is shown in Figure 2. Taking this as an example, because the network only has the main power supply for power supply, the current direction is that the system power supply flows to the load. When the fault occurs in the section, the traction network corresponding to the section monitors the fault current passing through, Thus, for the switch with fault over-current, the status value of the corresponding node is "1", whereas for the switch without fault over-current, the status value is "0". That is to say, for a single switch node, only the downstream section fault needs to be considered.

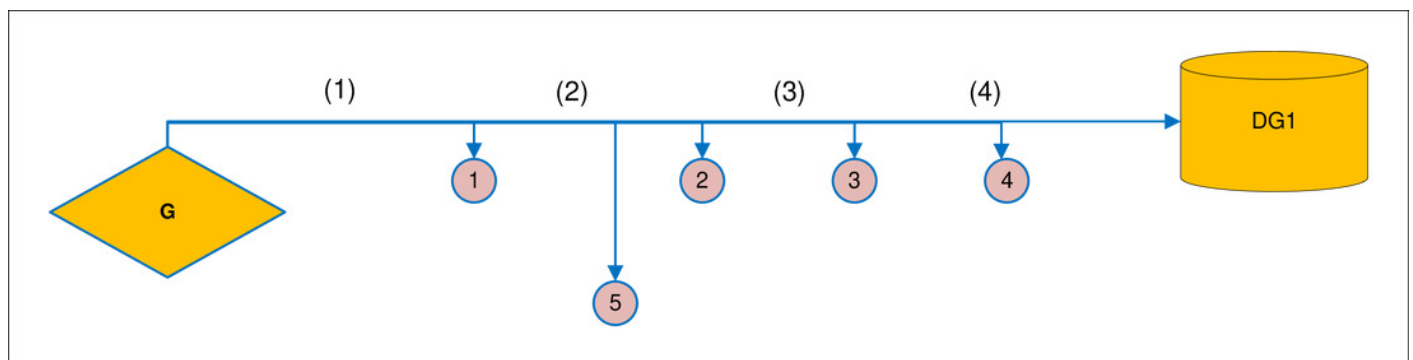


Figure 3

Figure 3. TPSSOA flow chart

TPSSOA firstly collects and uploads the fault current information in real time by using traction network, and realizes the conversion from fault current information to fault vector by using improved fault integer programming model, that is, according to the actual situation of fault current direction detected by traction network, it can be converted into "1", "- 1" or "0". Then the switch function of urban rail transit with rail transit is constructed, and the equivalent fault vector of fault location is calculated. The equivalent fault vector is input into the algorithm, the population dimension of PSO and the coding length of genetic algorithm are set as the total number of feeder sections, and the evaluation function is the objective function of the algorithm. Finally, the optimal particle position of PSO is output to realize the fault section location. In this paper, an adaptive PSO is proposed by dynamically improving the fitness value of the PSO. Combined with the adaptive genetic algorithm, the search iteration ability of the adaptive genetic PSO is proposed. The corresponding flow chart is shown in Figure 3.

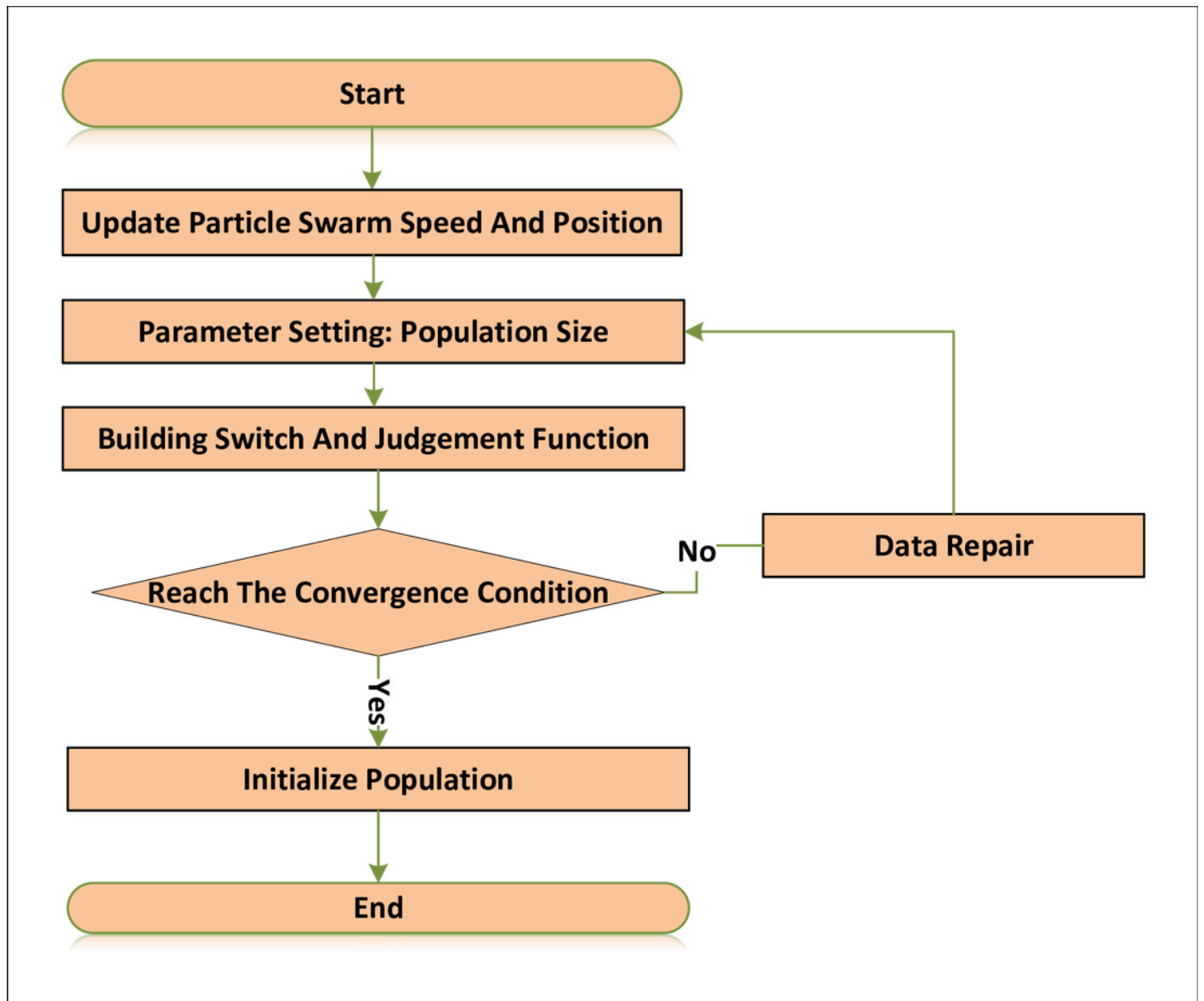


Figure 4

Figure 4. No distortion in single section

No distortion in single section The iterative curves of the two algorithms in fault location are shown in Figure 4 and Figure 5. The horizontal axis is the number of iterations, and the vertical axis is the fitness value. The default fault location is the feeder segment (1), and the fault information is not distorted. It can be seen from the results in Figure 4 that both algorithms can achieve minimum values within the maximum number of iterations, but the speed of TPSSOA is the fastest and IPSO is the slowest. The preset fault location is feeder section (2), and the fault information at switch (3) is distorted.

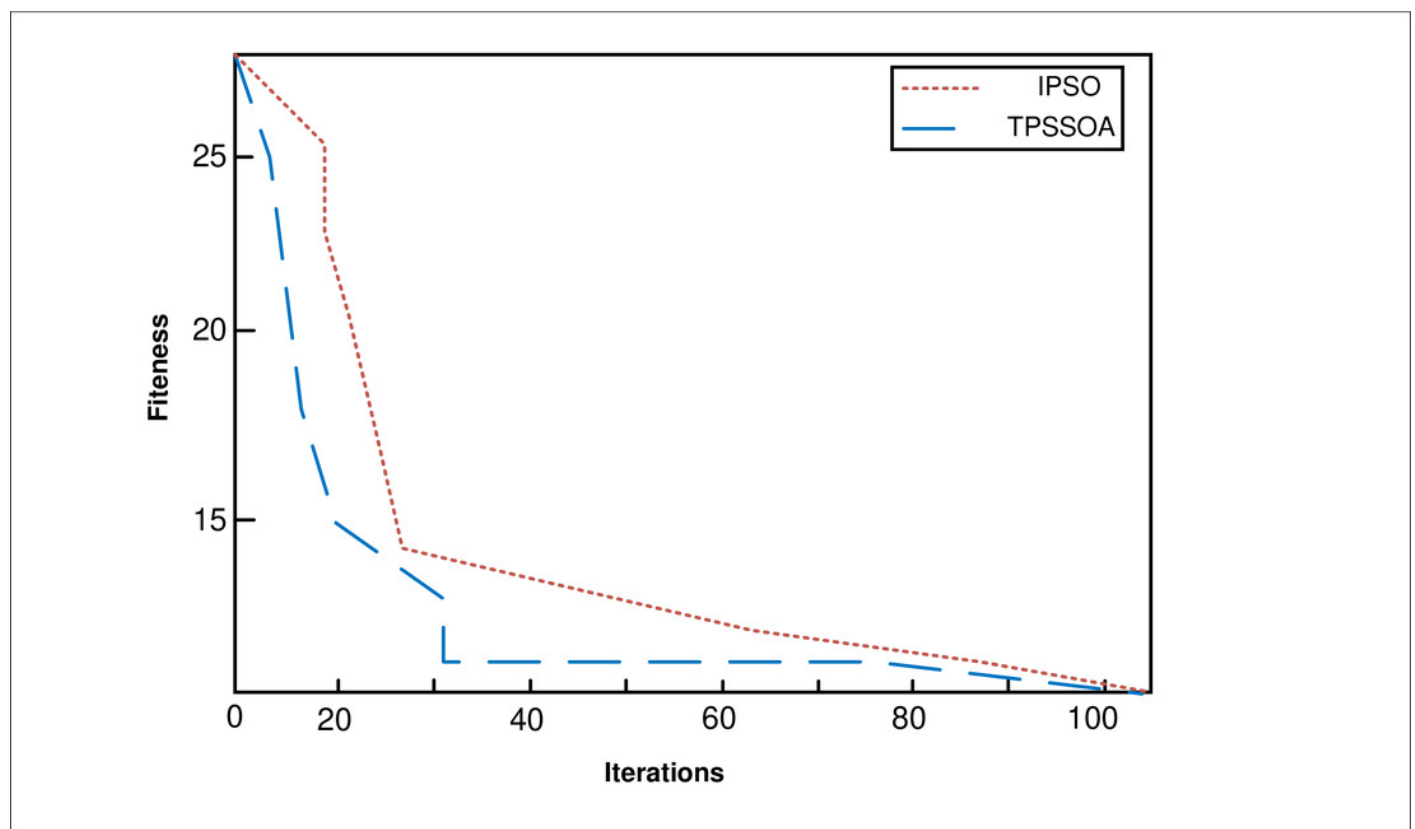


Figure 5

Figure 5. No distortion in multiple sections

The iterative curves of the two algorithms in fault location are shown in Figures 4 and 5. The horizontal axis is the number of iterations, and the vertical axis is the fitness value. The default fault location is the feeder segment (1), and the fault information is not distorted. It can be seen from Figure 5 that IPSO falls into a local optimal value at the early stage of iteration. In order to obtain the global optimal value, more iterations are needed. However, TPSSOA achieves global extremum with less iterations.

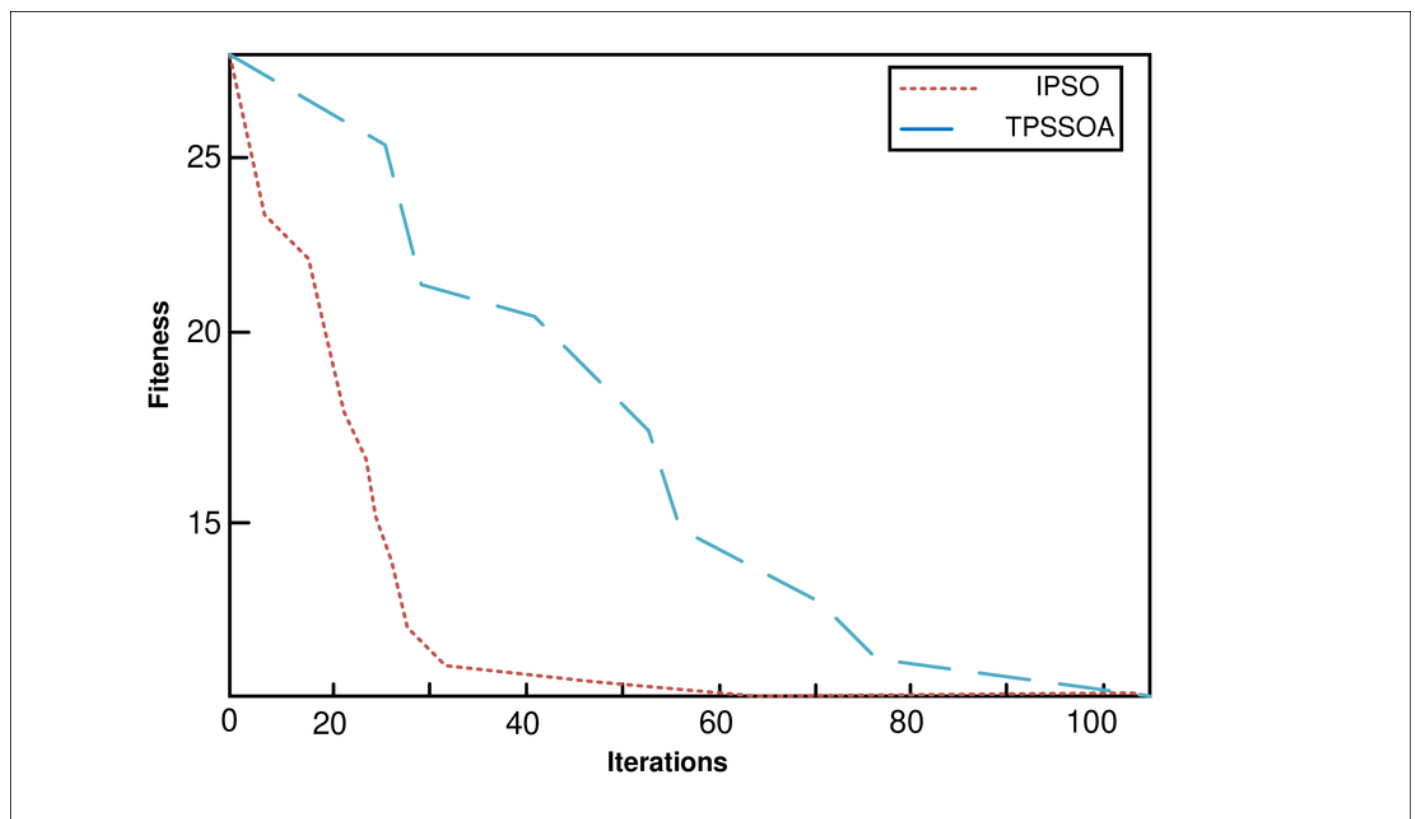


Table 1 (on next page)

Parameters of TPSSOA algorithm

The reference voltage of rail transit traction system used in this experiment is , the reference power is , and the network load is . The Parameters of TPSSOA algorithm is shown in table 1.

1

Table 1 Parameters of TPSSOA algorithm

Parameter	PSOA	DG	Testing sample
Population	45	51	35
Max Iterations	45	51	35
Dimension	61	23	/
Code length	76	23	25

2

Table 2 (on next page)

Table 2 DG access results

When DG is not connected, when there is no DG in urban rail transit, the status values of the switch are only "0" and "1". If there is high temperature, humidity and other harsh conditions, the fault information collected may be different from the actual value. Therefore, the information distortion is considered in this experiment. The simulation results are shown in Table 2. It can be seen from the results in Table 2 that the fault area can also be accurately located when multiple sections are in fault at the same time and the fault information is not accurate. At the same time, the fault section can be accurately determined even if the fault information of multiple feeder sections is not accurate. As a result of the simulations, the fault location method proposed can dynamically adapt to the flow of DGs into and out of the fault, and the experimental results are not disturbed by distorted information.

1
2

Table 2 DG access results

Fault	Equivalent fault vector	Output optimal solution	Node
Single fault	[110011010001100101001100]	[101011010001100101110000]	(1)
Multiple faults	[100011010001100101111101]	[111011010001100101111000]	(3)
Multiple information distortion	[111011010001100101111101]	[100011010001100101111100]	(2)

3
4